A 79-GHz Planar Antenna Array Using Ceramic-Filled Cavity Resonators in LTCC

Frank Bauer, *Student Member, IEEE*, and Wolfgang Menzel, *Fellow, IEEE*

***Abstract*—Design and measurement of a planar antenna array realized in low temperature co-fired ceramic (LTCC) are presented. The antenna elements are ceramic-filled cavity resonators fed by an integrated laminated waveguide network and a slot in each resonator. The antenna is designed to operate in the 79-GHz frequency range. The array shows good impedance matching and a stable radiation pattern within a bandwidth of approximately 5 GHz. The presented results of a first design show that the antenna is a promising candidate for 79-GHz automotive or related applications and ideally suited for LTCC integration.**

***Index Terms*—Low temperature co-fired ceramic (LTCC), millimeter-wave antenna arrays, substrate integrated waveguide (SIW), slotted waveguide antenna arrays.**

I. Introduction

IN ADDITION to the existing automotive frequency band from 76 to 77 GHz used for long-range radar (LRR) applications such as autonomous cruise control (ACC), the 79-GHz band (77–81 GHz) has been allocated by the European Commission in 2004 for future short- and mid-range (SRR, MRR) high-resolution automotive radar systems. Therefore, safety and comfort applications such as collision warning, blind spot detection, and precrash vehicle preparation [1] will benefit from higher sensor performance at smaller size compared to the established sensor technology at 24 GHz [2], [3]. Highly integrated SiGe transceiver chips [4], [5] minimize the number of RF transitions as a result of integration of multiple blocks, and therefore enable the realization of compact and low-cost systems, which are a prerequisite for mass-market applications. Sensor designs on low temperature co-fired ceramics (LTCCs) additionally offer low-cost 3-D multilayer integration, high mechanical stability, and better thermal conductivity, compared to traditional soft substrate materials. The design of planar wideband antennas on LTCC at millimeter waves, however, is a challenging task due to the high permittivity reducing the bandwidth and efficiency of radiating elements. In [6], we presented the application of traveling-wave microstrip grid array antennas within a 79-GHz LTCC-based radar sensor. Besides a wideband impedance matching, these antennas show a stable radiation pattern within a bandwidth of 2.5–3 GHz. Resonant slot array antennas based on laminated waveguide (LWG) in LTCC [7] show an even smaller bandwidth of approximately 2 GHz. Therefore, in order to cover the whole available frequency band between 76 and 81 GHz, antennas with higher bandwidth are necessary. In this letter, we present a planar antenna array using broadband radiating elements being completely integrated in LTCC.

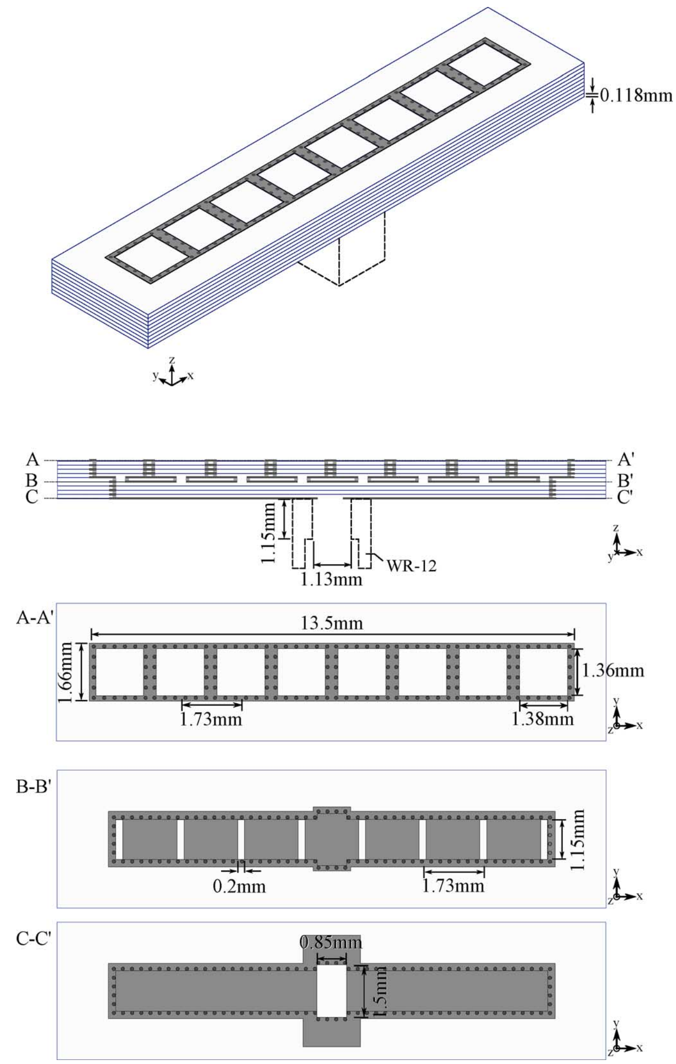

Fig. 1. Configuration of the proposed 79-GHz cavity resonator antenna array in LTCC.

II. Antenna Design

The overall structure of the proposed cavity resonator antenna array in an LTCC multilayer is shown in Fig. 1, comprising

Manuscript received May 14, 2013; revised June 23, 2013; accepted July 06, 2013. Date of publication July 11, 2013; date of current version August 02, 2013. This work was supported by the COMET K2 Center "Austrian Center of Competence in Mechatronics (ACCM)." The COMET program is supported by the Austrian Federal Government, the Federal State of Upper Austria, and the scientific partners of ACCM.

The authors are with the Institute of Microwave Techniques, University of Ulm, 89069 Ulm, Germany (e-mail: frank.bauer@uni-ulm.de; wolfgang.menzel@uni-ulm.de).

Color versions of one or more of the figures in this letter are available online at http://ieeexplore.ieee.org.

Digital Object Identifier 10.1109/LAWP.2013.2272914

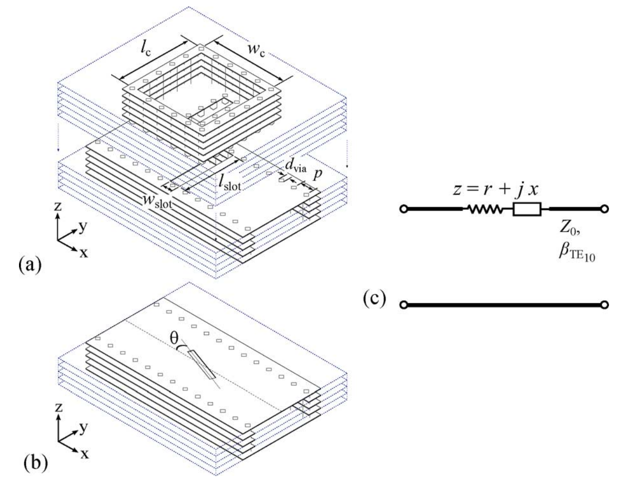

Fig. 2. (a) Slot-fed cavity resonator antenna element. (b) Standard inclined slot radiator element. (c) Equivalent circuit representation.

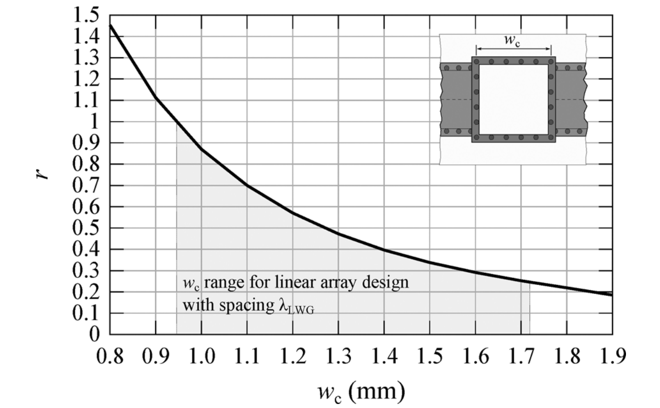

Fig. 3. Normalized resonant resistance at 79 GHz as function of cavity width w_c.

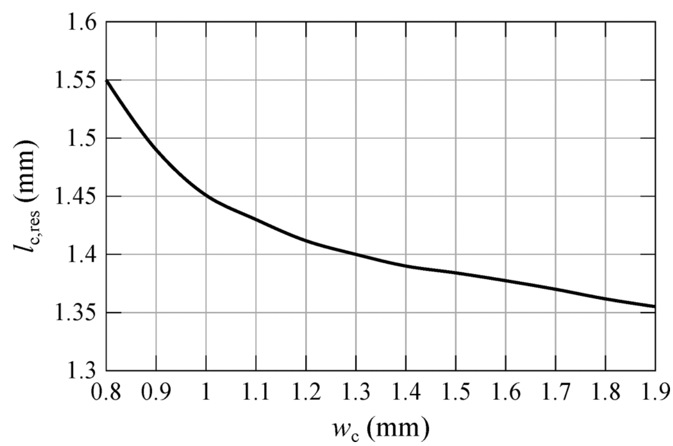

Fig. 4. Cavity length $l_{c,res}$ at resonance as a function of cavity width w_c.

nine ceramic layers of a sintered thickness $t = 0.118$ mm (TDK LTCC material with $\epsilon_r = 7.28$ and $\tan\delta = 0.006$ [8]). The radiating antenna elements consisting of ceramic-filled cavities are fed by transverse slots in the upper metallization of a LWG. The dimensions of the LWG are $a_{LWG} = 1.15$ mm and $b_{LWG} = 0.472$ mm (four layers of LTCC). According to the size of the cavities and the relatively short guided wavelength $\lambda_{LWG} = 1.73$ mm $= 0.456\lambda_0$ (with λ_0 as free-space wavelength at 79 GHz), the radiating elements are spaced λ_{LWG} apart from each other without generating unwanted grating lobes. A constant via diameter of $d_{via} = 0.1$ mm and via pitch of $p = 0.25$ mm are used throughout the design. Since the number of available layers was limited, the antenna is center-fed by a WR-12-LWG transition acting as power divider at the same time. Using more layers, the power splitting could also be achieved by an integrated LWG-power divider as presented in [6].

A. Radiating Antenna Element

The radiating element was designed to have the same radiation properties as an open-ended integrated waveguide with the dominant propagating mode being TE_{10}. An open-ended LWG radiator, however, suffers from high reflections at the dielectric–air interface due to the high permittivity of LTCC. In [9], this problem has been addressed by cutting air-cavities into the radiating aperture, thus reducing the effective permittivity within the aperture. In order to enable a simple manufacturing process, the proposed antenna element in this letter follows a different approach by using a rectangular ceramic-filled cavity resonator formed by a via-fence and four ceramic layers corresponding to a cavity height of approximately $(\lambda_{LWG})/(4)$.

The radiating element shown in Fig. 2(a) is fed by a transverse slot in the upper metallization of the LWG. Since the transverse slot interrupts the longitudinal currents (x-direction) in the top metallization of the LWG, an element near resonance can be modeled as a normalized series impedance, the value of which can be derived from the scattering coefficient S_{11} using the following equation:

$$z = r + jx = \frac{2 \cdot S_{11}}{(1 - S_{11})}. \quad (1)$$

This approach is known from inclined center line slots as shown in Fig. 2(b) [10]. The normalized impedance is dependent on the slot geometry and cavity size. Since standard screen-printing is applied at the inner metallization layers, the dimensions of the slot feeding the cavity element are subject to certain geometrical restrictions and are therefore set to a fixed width $w_{slot} = 0.2$ mm and a length $l_{slot} = 1.15$ mm corresponding to the width of the LWG. At resonance, the impedance assumes a real value that is referred to as normalized resonant resistance r. For the proposed radiating element, the value of r can be adjusted by changing the width of the cavity w_c. A plot of computed values of r as a function of cavity width w_c is shown in Fig. 3 with the normalized resistance at resonance being inversely proportional to the cavity width. The corresponding cavity lengths $l_{c,res}$ at resonance are given in Fig. 4. In order to show the capabilities of the proposed radiating element, Fig. 5 depicts real and imaginary parts of the normalized impedance z of a cavity resonator over frequency in comparison to an inclined slot. It can be seen that the impedance variation of the cavity resonator antenna element is very flat, and therefore its bandwidth is significantly higher compared to a standard inclined slot.

B. Array Design and Feeding Transition

Since the intended element spacing within the linear array is $\lambda_{LWG} = 1.73$ mm, this value also represents the maximum possible cavity width. At the given dimensions of the coupling slot,

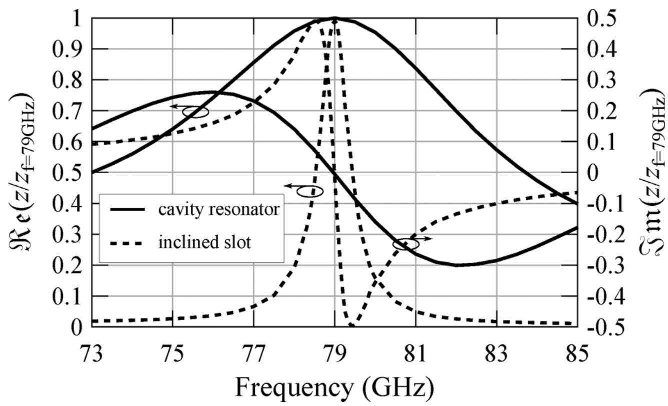

Fig. 5. Normalized impedance of a cavity resonator element in comparison to a standard inclined slot.

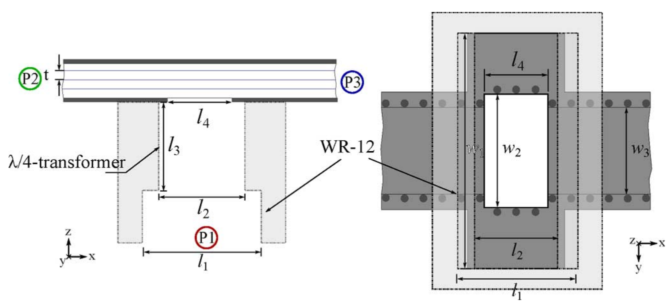

Fig. 6. Bottom and cross-section view of broadband WR-12 to LWG feeding transition. Design parameters: $w_1 = 3.1$ mm, $w_2 = 1.5$ mm, $w_3 = 1.15$ mm, $l_1 = 1.55$ mm, $l_2 = 1.13$ mm, $l_3 = 1.15$ mm, $l_4 = 0.85$ mm, $t = 0.118$ mm.

this corresponds to a minimal achievable normalized resistance of $r = 0.25$ (cf. Fig. 3). Hence, a center-fed eight-element array antenna with two branches was designed. With the element impedances combining in series, each LWG branch has to fulfill the matching condition

$$\sum_{n=1}^{4} z_n = 1. \quad (2)$$

The presented antenna uses identical elements. Due to the presence of pronounced mutual coupling between them, the initially obtained values from Figs. 3 and 4 have to be optimized. In general, this can be done by determining the mutual impedances between the elements and adjusting the individual elements accordingly [11]. However, due to the small size of the presented array, the final optimization of the antenna was performed using a full-wave finite-difference time-domain (FDTD) analysis including the feeding structure depicted in Fig. 6. As already mentioned above, the feeding structure serves as transition and power divider at the same time. For an improved matching, a quarter-wavelength WR-12-waveguide section with reduced height is used (cf. Fig. 6). The simulated S-parameters (port numeration according to Fig. 6) given in Fig. 7 show a symmetric splitting and a return loss greater than 15 dB between 74 and 82 GHz. Due to the aperture coupling, Ports 2 and 3 have an inherent 180° phase shift that is necessary for an in-phase excitation of the radiating elements in both branches.

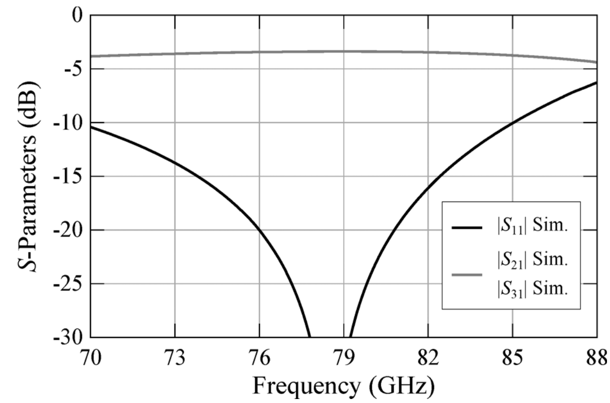

Fig. 7. Simulated S-parameters of the WR-12–LWG power splitting transition.

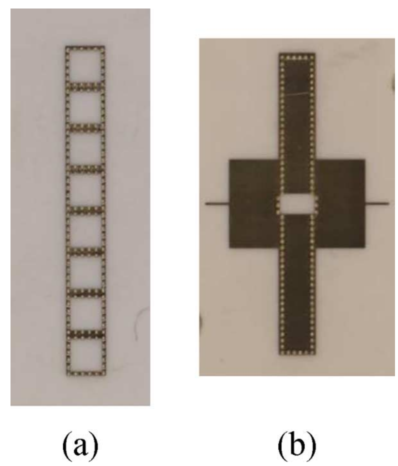

Fig. 8. Photograph of the cavity resonator antenna array. (a) Top. (b) Bottom.

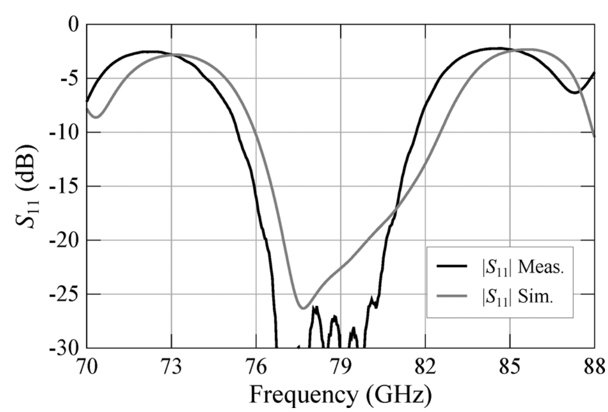

Fig. 9. Measured and simulated reflection coefficient of the cavity resonator antenna array.

III. Measurement Results

The reflection coefficient of the fabricated antenna (Fig. 8) is presented in Fig. 9 and shows a measured impedance bandwidth (return loss greater 10 dB) of 6.5 GHz that is in good agreement with the simulated results. The measured radiation patterns in E- and H-plane are also in good agreement with simulation as shown in Figs. 10–12. Over the whole operating bandwidth from 76 to 81 GHz, the antenna shows a stable radiation pattern with a 3-dB beamwidth of 13° in the E-plane and a maximum measured sidelobe level of -11 dB occurring at 81 GHz.

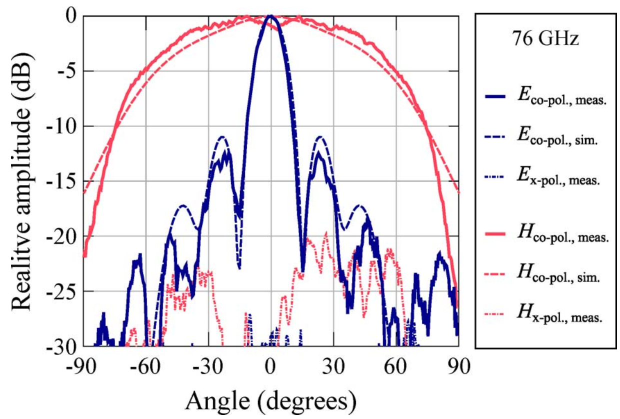

Fig. 10. Measured and simulated radiation diagram of the cavity resonator antenna array at 76 GHz.

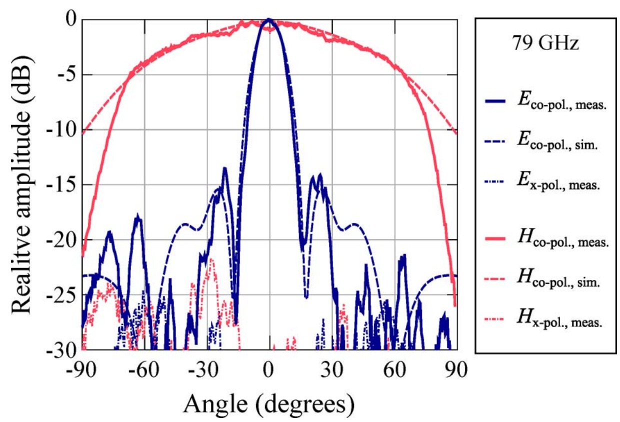

Fig. 11. Measured and simulated radiation diagram of the cavity resonator antenna array at 79 GHz.

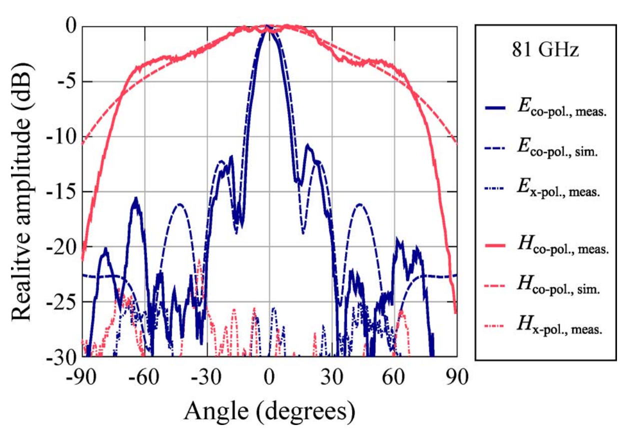

Fig. 12. Measured and simulated radiation diagram of the cavity resonator antenna array at 81 GHz.

In the H-plane, the 3-dB beamwidth is approximately 100°. Furthermore, the antenna shows a low measured cross-polarization level being more than 25 dB below the copolarization in the vicinity of the boresight direction. The measured gain at 79 GHz is 13.2 dBi. Fig. 13 shows the measured gain over frequency with a variation of 0.8 dB within the operating bandwidth of 5 GHz. With a directivity of 15.1 dBi, the antenna has

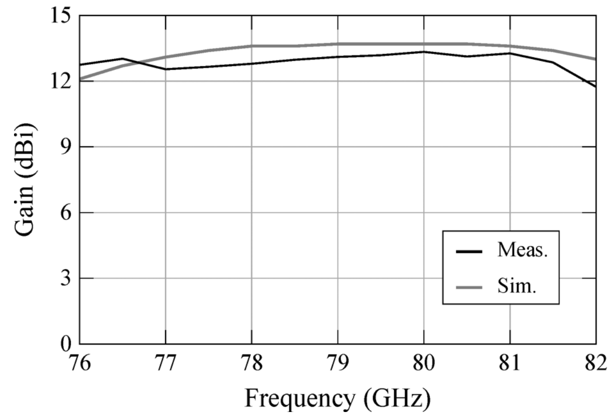

Fig. 13. Measured and simulated gain of the resonant cavity antenna array at boresight.

an efficiency of 65%. This value could be improved in future designs by using LTCC material with lower loss.

IV. Conclusion

An eight-element cavity resonator antenna has been presented. In high-permittivity material as LTCC, the cavity resonator element shows only a small impedance variation over frequency compared to a standard radiating slot within an LWG. Therefore, the measured results of the antenna show a wide operating bandwidth in terms of impedance matching and pattern stability being able to cover the whole frequency range from 76 to 81 GHz.

References

[1] K. Strohm, H.-L. Bloecher, R. Schneider, and J. Wenger, "Development of future short range radar technology," in *Proc. EuRAD*, Oct. 2005, pp. 165–168.

[2] H. Rohling, "Development milestones in 24 GHz automotive radar systems," in *Proc. 11th IRS*, 2010, pp. 1–5.

[3] I. Gresham, A. Jenkins, R. Egri, C. Eswarappa, N. Kinayman, N. Jain, R. Anderson, F. Kolak, R. Wohlert, S. Bawell, J. Bennett, and J.-P. Lanteri, "Ultra-wideband radar sensors for short-range vehicular applications," *IEEE Trans. Microw. Theory Tech.*, vol. 52, no. 9, pp. 2105–2122, Sep. 2004.

[4] S. Pacheco, R. Reuter, S. Trotta, D. Salle, and J. John, "SiGe technology and circuits for automotive radar applications," in *Proc. 11th IEEE SiRF*, Jan. 2011, pp. 141–144.

[5] H. Forstner, H. Knapp, H. Jager, E. Kolmhofer, J. Platz, F. Starzer, M. Treml, A. Schinko, G. Birschkus, J. Bock, K. Aufinger, R. Lachner, T. Meister, H. Schafer, D. Lukashevich, S. Boguth, A. Fischer, F. Reininger, L. Maurer, J. Minichshofer, and D. Steinbuch, "A 77 GHz 4-channel automotive radar transceiver in SiGe," in *Proc. IEEE RFIC*, Apr. 2008, pp. 233–236.

[6] F. Bauer, X. Wang, W. Menzel, and A. Stelzer, "A 79-GHz radar sensor in LTCC technology using grid array antennas," *IEEE Trans. Microw. Theory Tech.*, vol. 61, no. 6, pp. 2514–2521, Jun. 2013.

[7] F. Bauer and W. Menzel, "A 79-GHz resonant laminated waveguide slotted array antenna using novel shaped slots in LTCC," *IEEE Antennas Wireless Propag. Lett.*, vol. 12, pp. 296–299, 2013.

[8] S. Brunner, M. Stadler, X. Wang, F. Bauer, and K. Aichholzer, "Advanced high frequency LTCC technology for applications beyond 60 GHz," in *Proc. 8th CICMT*, Erfurt, Germany, Apr. 2012, pp. 77–81.

[9] B. Sanadgol, S. Holzwarth, A. Milano, and R. Popovich, "60 GHz substrate integrated waveguide fed steerable LTCC antenna array," in *Proc. 4th EuCAP*, 2010, pp. 1–4.

[10] S. Rengarajan, "Scattering characteristics of a centre-inclined slot in a broad wall of a rectangular waveguide," *Inst. Elect. Eng. Proc. H, Microw., Antennas Propag.*, vol. 137, no. 6, pp. 343–348, 1990.

[11] T. Bird, "Analysis of mutual coupling in finite arrays of different-sized rectangular waveguides," *IEEE Trans. Antennas Propag.*, vol. 38, no. 2, pp. 166–172, Feb. 1990.